Proceedings of the First International Conference on Press-in Engineering 2018, Kochi

3-D Behaviour of Coastal Dyke Installed by Double Sheet-piles with Partition Wall

Kakuta FUJIWARA
Assistant Manager, Construction Products Development Division, Nippon Steel & Sumitomo Metal Corporation, Tokyo, Japan
Email: fujiwara.8fa.kakuta@jp.nssmc.com
Shinji TAENAKA
Senior Researcher, Steel Structures Research Laboratories, Nippon Steel & Sumitomo Metal Corporation, Chiba, Japan
Kousuke TAKAHAMA
Student, Faculty of Engineering, Gifu University, Gifu, Japan
Atsushi YASHIMA
Professor, Faculty of Engineering, Gifu University, Gifu, Japan

ABSTRACT

In the near future, there is fear that coastal dykes will sink by liquefaction due to a large earthquake such as Nankai Trough Earthquake. To overcome the potential damage, the application of double sheet-piles with partition walls to coastal dyke has been proposed. The partition wall is installed perpendicular to the double sheet-piles with a certain interval. Authors confirmed that this structure should be effective in reducing the settlement of coastal dyke on liquefied ground through the model tests. To propose a design method for the double sheet-piles with partition walls countermeasure, the authors carried out 2-D numerical analyses (code:LIQCA2D15) based on the model tests. As a result, good reproducibility of dyke behaviour such as settlement, sheet-pile deformation and excess pore water pressure could be confirmed. However, the applicability of numerical analyses was only discussed in 2-D framework. Therefore, in this study, authors discussed the 3-D behaviour of this structure using 3-D numerical analyses (code:LIQCA3D15). It was found that the wider the interval of partition walls becomes, the larger the bending deformation of sheet piles as well as the settlement of coastal dyke itself become.

Key words: *Coastal dyke, Earthquake, Liquefaction, Sheet-pile, Reinforcement*

1. Introduction

Several coastal dykes collapsed due to shaking and tsunami caused during the 2011 off the Pacific coast of Tohoku Earthquake (Oka *et.al.* 2012). A Large subduction-zone earthquake such as Nankai Trough Earthquake is also concerned to occur in the near future (Cabinet Office 2015). As a countermeasure against a large earthquake and tsunami, installing double sheet-piles into a dyke has been proposed. For the enhancement of the effectiveness this countermeasure, the double sheet-piles with partition walls have been investigated, as shown in **Fig. 1** (Fujiwara 2017).

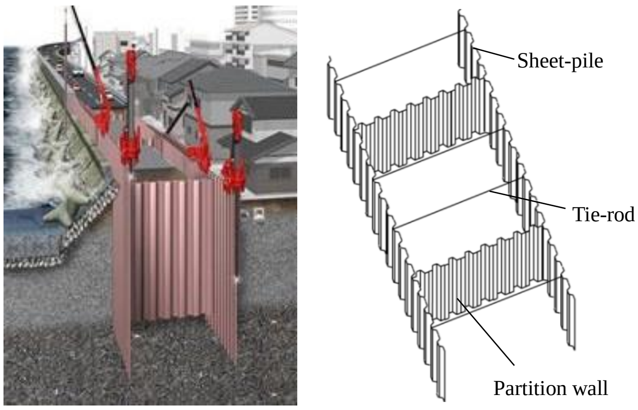

(a) Construction situation (b) Sheet-piles structure

Fig. 1 Schematic of the reinforced coastal dyke

The partition walls are sheet-pile walls that are installed perpendicular to the double sheet-piles. The effectiveness of this countermeasure against earthquake has been studied through model tests and numerical analyses. The authors confirmed that dyke settlement due to ground liquefaction should be reduced remarkably. In addition, since sheet-piles keep their height, sheet-piles even without partition walls prevent tsunami from overflowing (Furuichi. *et.al.* 2015). However, the design method of this countermeasure has been proposed only in a 2-D framework (Fujiwara *et.al.* 2017). As the double sheet-piles with partition walls have a 3-D structure, the behavior of coastal dykes with countermeasure should be confirmed in a 3-D framework. For an example of Kochi coastal dyke, partition walls are generally spaced approximately every 9 m conventionally. In this study, the authors carried out 3-D numerical analyses as a basic study to propose a design method. First, shaking model tests were conducted to verify the validity of the numerical models.

2. Overview of model tests

2.1. Test procedures

The shaking table model tests were carried out under a gravity field. The model ground consisted of a dyke, liquefiable and unliquefiable layers. The height of the model dyke was 300 mm. That condition is approximately 1/25 geometrical scale to the actual structure. As shown in **Table 1**, three cases: Case-A (without countermeasure), Case-B (with double sheet-piles), and Case-C (with double sheet-piles and partition wall), were examined. The ground and sheet-pile conditions are shown in **Table 1**. The model sheet-pile and partition wall were steel plates with thickness of 3.2 mm and 2.3 mm, respectively based on the similarity rule (Iai. 1988). The tops of double sheet-piles were connected with tie-rods. The side of the partition wall was welded to double sheet-piles. The partition walls were installed at a gap of 340 mm for the extension of dyke direction (equal to approximately 9m in an actual structure). More detailed experimental conditions can be found in the literature (Fujiwara *et.al.* 2017). The wave recorded at Kamaishi during the 2011 off the Pacific coast of Tohoku Earthquake was adjusted as the input earthquake motion for shaking model tests, considering the similarity rule. In this study, input earthquake motion was modified by extending the observed time duration three times to emphasize the effect of countermeasures (**Fig. 2**).

2.2. Test results

Deformed configuration of Case-C after shaking is shown in **Fig. 2**. While the foundation ground deformed due to liquefaction, the settlement of double sheet-piles themselves and the ground inside sheet-piles are reduced significantly. The settlements at two points along the extending direction of the dyke are shown in **Fig. 2 (C)**, and these both values were approximately 10mm. Therefore, the behavior of dyke settlement was almost constant along extending direction. The time history of the settlement at the top of the dyke in Cases-A~C is shown in **Fig. 3.** The residual settlement in Case-C was 10% and 24% compared to Case-A and B respectively.

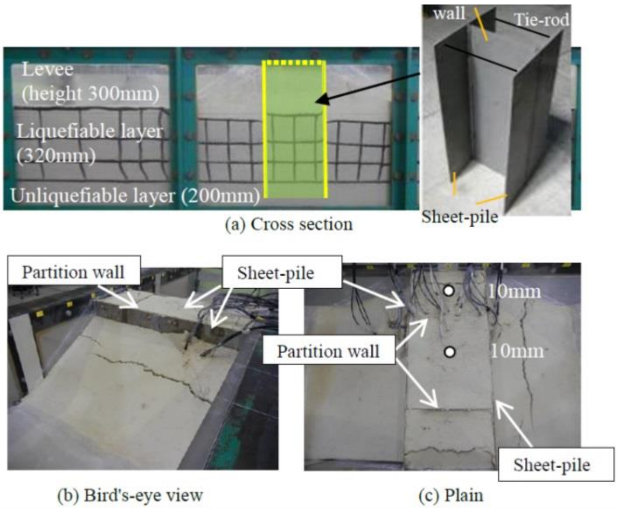

(a) Cross section (b) Bird's-eye view (c) Plain

Fig. 2 Test results

Table 1. Soil conditions and countermeasures

Test cases	Soil conditions							Countermeasures				
	Levee	Liquefiable layer			Unliquefiable layer			Sheet-pile		Tie-rod	Partition-wall	
	γ_t (kN/m^3)	γ_t (kN/m^3)	D_r (%)	k (m/sec)	γ_t (kN/m^3)	D_r (%)	k (m/sec)	t (mm)	L (mm)	ϕ (mm)	t (mm)	L (mm)
Case-A	16.2	19.1	42.4		19.9	91.4		—	—	—	—	—
Case-B	15.6	19.0	43.2	2.0×10^{-5}	19.7	91.2	7.2×10^{-6}	3.2	720	4.0	—	--
Case-C	16.0	19.1	44.4		19.8	92.7		3.2	720	4.0	2.3	720

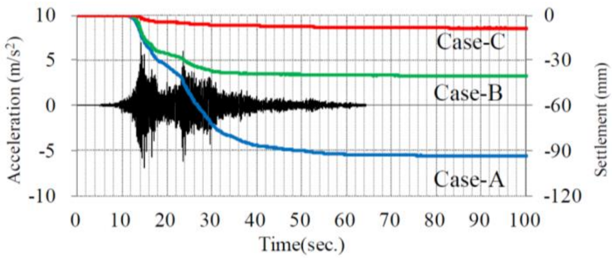

Fig. 3 Input motion and settlement

The very satisfactory settlement reduction effect was confirmed by the double sheet-piles with a partition wall.

3. Numerical analysis

3.1. Outline of the Numerical Code, LIQCA

We will discuss the reproducibility of numerical analyses in this chapter. In this study, we use a three-dimensional program, LIQCA3D15 (LIQCARI. 2015). The governing equations for coupling problems between the soil skeleton and pore water pressure were formulated based on the two-phase mixture theory (Biot. 1962) and u-p (displacement of solid-phase and pore water pressure) formulation was adopted in 3-D analysis. The finite element method (FEM) was employed for spatial discretization of the equation of motion, whereas the finite difference method (FDM) (Oka *et.al.* 1994) was employed for spatial discretization of pore water pressure in the continuity equation. In this simulation, a cyclic elastic-plastic model (Oka *et.al.* 1999) was applied to the coastal dyke with liquefiable layer.

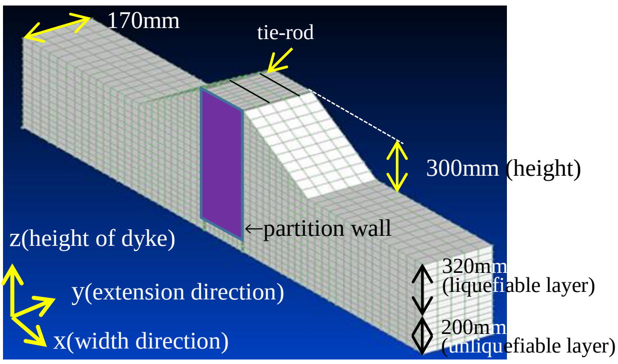

Fig. 4 Numerical model (Case-C)

3.2. Conditions for numerical model

The size of the numerical model (i.e. width of the ground, thickness of layers, etc) is basically equal to the conditions of the model tests, as shown in **Fig. 4**. However, the extension direction of the dyke is 170mm which is half of the model test container due to the symmetric nature along the extension direction of the dyke. The displacements of the bottom boundary are fixed in all directions. The horizontal displacement of side boundaries is also fixed.

The dyke and liquefiable layer are modeled by a cyclic elasto-plastic model, and the unliquefiable layer is modeled by the Ramberg-Osgood model (Ramberg *et.al.* 1943). The material parameters for the cyclic elastic-plastic model are summarized in **Table 2**. The parameters for the liquefiable layer were determined by considering the results of undrained cyclic triaxial compression tests. The stress strain relation, effective stress path and liquefaction resistance curve are shown as **Fig. 5**. Since the double sheet-piles did not yield for the model tests, double sheet-piles are modeled by a solid elastic material. A joint element in which the slipping and separation are taken into account is not used between the ground and sheet-pile in this model. The tie-rod and partition wall are not modeled by the element itself but modeled by the displacement constraint condition of nodes. The interval of tie-rod in the extension direction of the dyke is 113 mm. The nodes on both side ends of tie-rod are put on the nodes of the sheet-piles in the same position and they are given equal displacement boundary conditions in the vertical and horizontal directions.

Table 2. Material parameters for liquefiable layer

Initial void ratio	e	0.813
Compression index	λ	0.015
Swelling index	κ	0.002
Initial shear modulus ratio	G_0/σ_{m0}	1000
Phase transformation stress ratio	M^*_m	0.909
Failure stress ratio	M^*_f	1.122
Reference strain parameter	γ_P	0.01
Reference strain parameter	γ_E	0.02
Hardening parameter	B_0	7000
Hardening parameter	B_1	50
Hardening parameter	C_f	0
Dilatancy parameter	D_0	3
Dilatancy parameter	n	3
Anisotropy parameter	C_d	2000

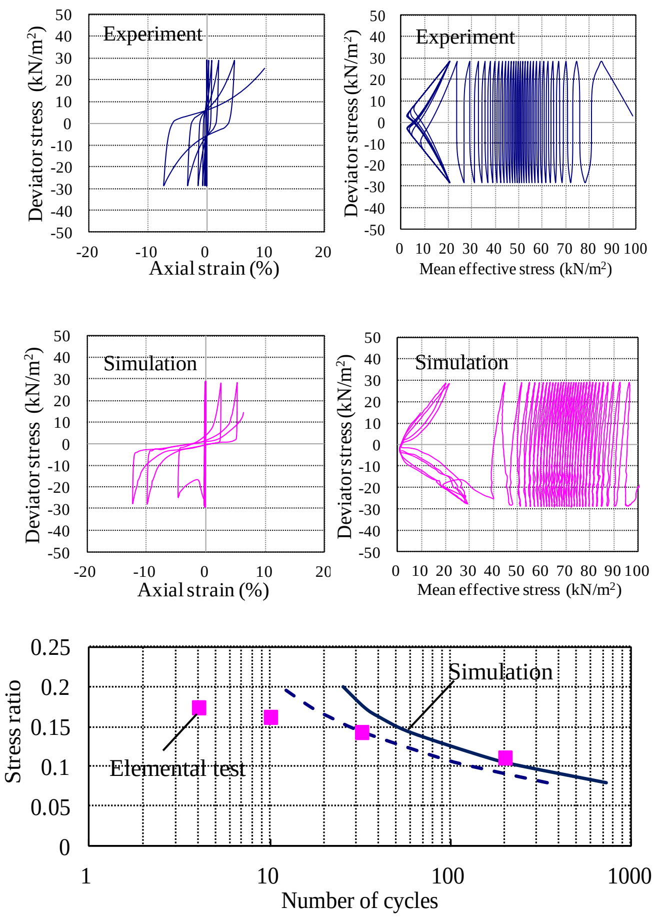

Fig. 5 Elemental tests

As far as the movement of the partition wall is concerned, the equal-displacement conditions in all directions are set for all nodes located on the partition wall. Therefore, shear and bending deformations are not allowed for the partition wall.

Boundary conditions are as follows:

A) The bottom of the ground is fixed in the horizontal and vertical direction.

B) The side boundary of model is fixed in the horizontal direction.

C) The water level is adjusted to the surface of the liquefiable layer.

D) The drainage boundary is set on the surface of the liquefiable layer.

E) The bottoms of sheet-piles are given free condition same as experimental ones.

The input wave is shown as **Fig. 3**. The incremental time interval is 0.002 seconds, the coefficient β of the Newmark method is set at 0.3025, and γ is set at 0.6. For Rayleigh damping, a proportional type to the initial stiffness is used. The coefficient is set at 0.003 which corresponds to the 3.0% damping factor to the first natural period of 0.3 seconds of the level ground portion.

3.3. Verification of reproducibility

For Case-A ~ C, the dyke deformation together with excess pore water pressure ratio distribution (t=80sec.) are shown in **Fig. 6**. As soil conditions were uniform across the test model, the deformations of dyke and ground caused by liquefaction were symmetrical, as shown by the model tests.

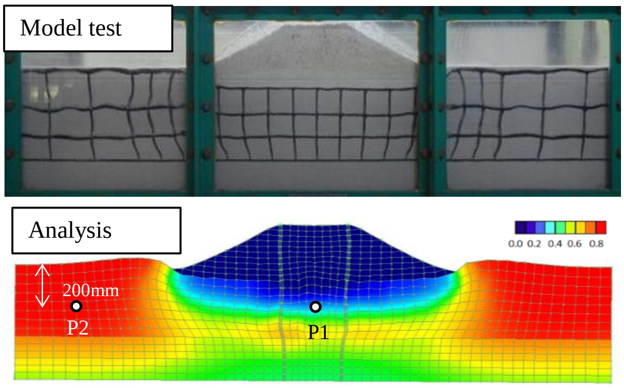

(a) Case-A

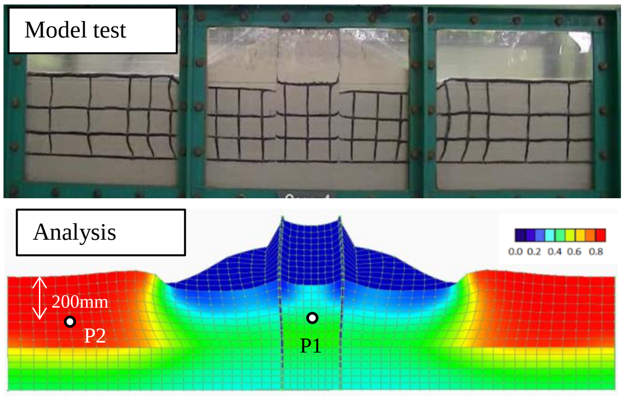

(b) Case-B

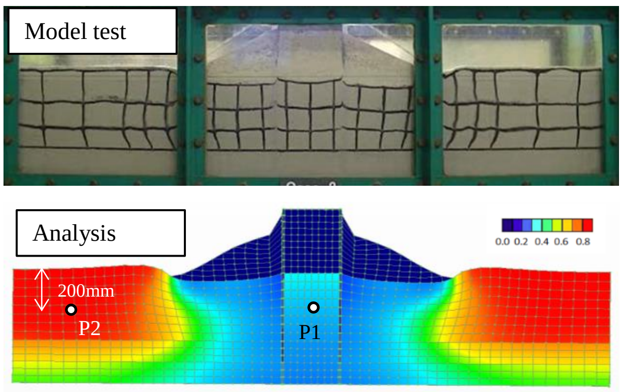

(c) Case-C

Fig. 6 Excess pore water pressure ratio distribution in deformed mesh

The result of Case-A reproduced the behavior of the model tests in which the horizontal ground was liquefied and the ground beneath the dyke flowed laterally, causing the dyke to settle while spreading horizontally.

For Case-B and C, although the dyke settled and deformed due to liquefaction, sheet-piles and partition walls did not settle because the bottom end of sheet-pile is installed into the unliquefiable layer. It is thought that the sheet-piles can protect the landside area from tsunami caused by earthquakes. The settlement of dyke surrounded by sheet-piles was reduced because the sheet-piles restricted deformation. Especially for Case-C, the enhancement of the performance of partition walls for reducing the settlement of dykes was confirmed.

For Case-A ~ C, the time histories of the vertical displacement at the top of dyke are shown in **Fig. 7**. Numerical analyses can reproduce quantitatively for Case-A and B. In contrast, the predicted settlement in Case-C is thought to be smaller than test results. This is because settlement due to slipping and separating is not reproduced without joint element.

For Case-A ~ C, the time histories of the excess pore water pressure at points P1 (beneath the dyke, **Fig. 6**) and P2 (horizontal ground, **Fig. 6**) are shown in **Fig. 8**. Although the ground at P2 liquefied, the excess water pore pressure at P1 did not reach the initial effective stress. It is found that numerical analyses reproduced such behaviors qualitatively. As the excess pore water pressure at P1 did not correspond well, it should be improved in the future work.

For Case-B and C, the sheet-pile deformation at t=80sec. are shown in **Fig. 9**. For Case-B, sheet-piles bended toward outside supported by top (tie-rods) and bottom (unliquefiable layer) in both analyses and model tests. The horizontal displacement of the bottom of sheet-piles are little in analyses. This is thought that the Ramberg-Osgood model applied for unliquefiable layer estimated soil harder than that in model tests. No dilatancy is considered in the Ramberg-Osgood model, this model is applicable to dense sand and clays in which little excess pore water pressure builds up. Though the unliquefiable layer made of dense sand (Dr=90%), the model applied for unliquefiable layer should be reconsidered. For Case-C, the results at the intermediate location of neighboring partition walls (y=170mm) are also plotted.

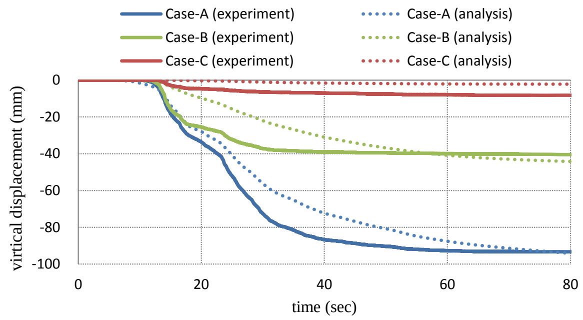

Fig. 7 Time histories of vertical displacement

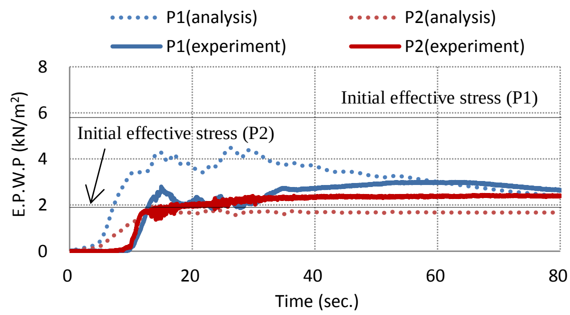

(a) Case-A

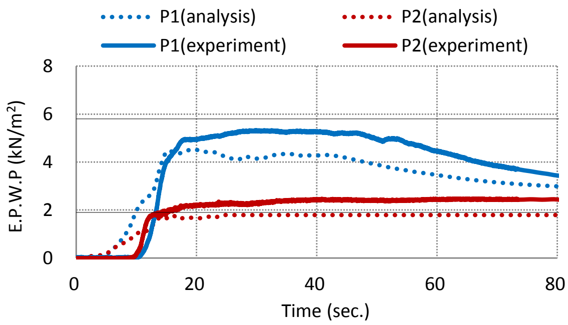

(b) Case-B

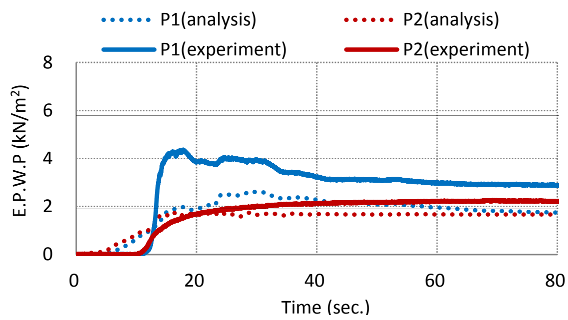

(c) Case-C

Fig. 8 Time histories of settlement at top of dyke

In both the analysis and experiment, sheet-piles exhibited little deformation.

From the abovementioned results, although the proposed numerical model needs some improvements, it almost can simulate deformation and settlement of dyke quantitatively. We decided to use this numerical model to investigate the behavior of the double sheet-piles with a

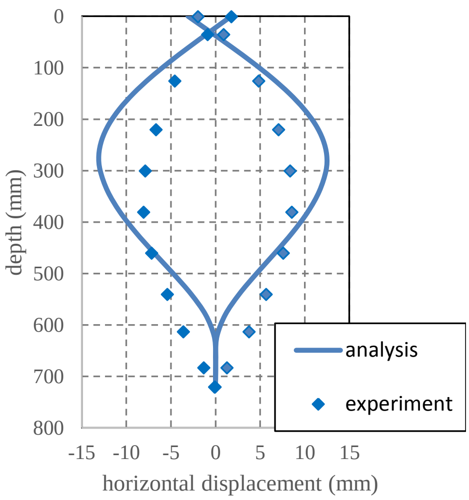

(a) Case-B

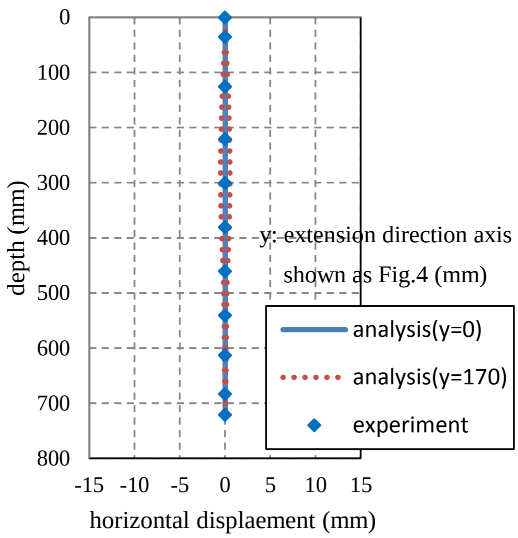

(b) Case-C

Fig. 9 Horizontal displacement of sheet-piles

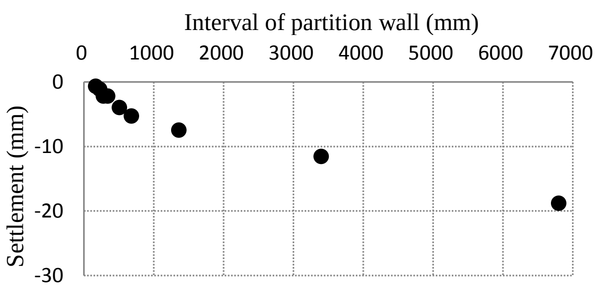

Fig. 10 Settlement of levee vs. interval of partition wall

partition wall structure.

3.4. Influence of the interval of partition walls

In Case-C, it is expected that the larger the interval of partition walls is, the more vertical settlement at top of dyke surrounded by sheet-piles and partition walls will be.

The interval of partition walls was varied under the condition in which all other numerical conditions were the same as those employed in the previous chapter. The intervals employed for parametric studies are 170, 226, 280, 510, 680, 1360, 3400 and 6800mm.

The relationship between the settlement of the top of dyke at t=80sec. and the interval of partition wall is shown in **Fig. 10**. It is found that the larger the interval of partition wall becomes, the more settlement of top of dyke will be.

The horizontal deformations of the sheet-piles at different distance from the partition wall are shown in **Fig. 11** for cases of the interval of partition wall with 170mm and 6800mm. The value of "y" in **Fig. 4** represents the distance from the partition wall. It is understood that the horizontal deformation becomes larger if the interval of a partition wall becomes larger by comparing the results shown in **Fig. 11**. It is found that a large vertical displacement of dyke is caused by a large horizontal deformation of a sheet-pile. A small horizontal deformation of a sheet-pile just beneath the top of dyke at y=3400mm is due to the existence of tie-rod.

The time histories of excess pore water pressures at points P1 (beneath the dyke, **Fig. 6**) and P2 (horizontal ground, **Fig. 6**) are shown in **Fig. 12** for cases of the interval of partition wall with 170mm, 340mm and 6800mm, respectively. There is no difference of excess pore water pressure generation for all cases at point P2. In contrast, at P1, while the excess pore water pressure generations for all cases almost coincide each other before t=15sec. The dissipation of the excess pore water pressure for narrower interval case is faster than that for wider internal case after t=15sec. The time histories of the maximum opening of a sheet-pile at the intermediate location of neighboring partition walls are plotted in **Fig. 13**. There is no difference in the increase in the opening of the sheet-pile for all cases before t=15sec. In contrast, the opening of the sheet-pile for a wider interval case is more than that for narrower case after t=15sec. The large opening of the sheet-pile induces the expansion of the soil surrounded by sheet-piles. The fast dissipation of excess pore water pressure is partly due to the expansion of soil

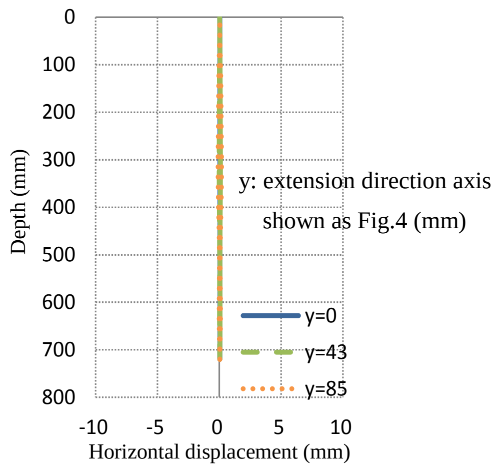

(a) interval of 170mm

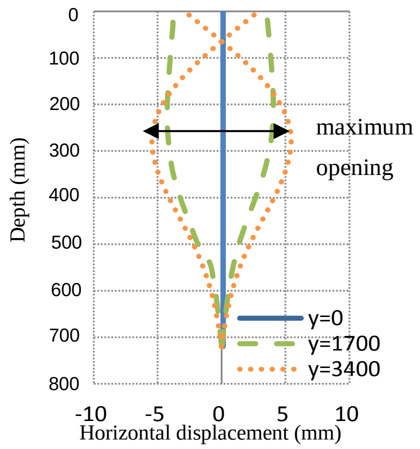

(b) interval of 6800mm

Fig. 11 Horizontal deformation of sheet-piles

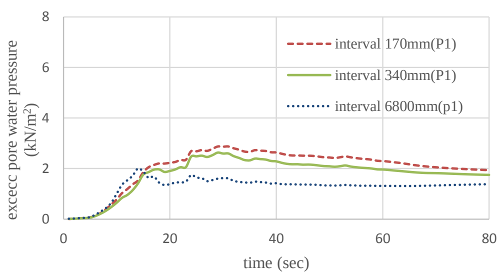

(a) P1

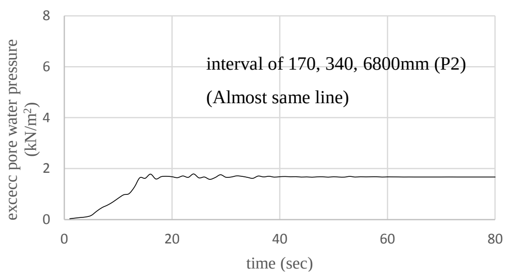

(b) P2

Fig. 12 Time histries of excess pore water pressure

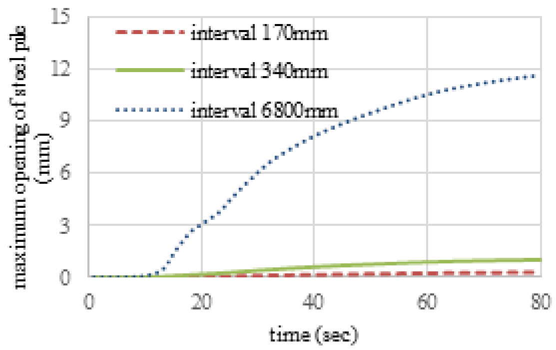

Fig. 13 Time histories of the maximum opening of sheet-piles

surrounded by sheet-piles. This typical three dimensional deformation characteristic can only be explained by 3-D analysis. As the slippage between the partition wall and soil was not allowed, the settlements for the cases with the interval of 170, 226 and 280 were underestimated.

4. Conclusions

Authors investigated the effectiveness of double sheet-piles with a partition wall as coastal dyke reinforcement method. The following conclusions were obtained by carrying out model tests and 3-D numerical analyses (code: LIQCA3D15).

1) Although the numerical model needs some improvements, it almost can simulate deformation and settlement of dyke quantitatively. Authors decided to use this numerical model to investigate the behavior of the double sheet-piles with a partition wall structure.

2) Through the parametric study focusing on the interval of partition walls, authors confirmed with an increase in the interval of the partition walls,

・the settlement of coastal dyke increased

・the bending deformation of the double sheet-piles increased

・the excess pore water pressure of the ground enclosed by double sheet-piles and partition walls decreased

3) For the improvement of the reproducibility of the numerical model, joint elements in which the slipping and separation are taken into account should be used between the ground and sheet-pile in the future study.

References

Biot, M. 1962. Mechanics of deformation and acoustic propagation in porous media, Journal of Applied Physics, 33 (4).

Cabinet Office., Government of Japan. 2015. Disaster management in Japan, p. 15.

Fujiwara, K. 2017. Reinforcement method for coastal dyke using double sheet-pile against large earthquake, Doctoral dissertation. (in Japanese)

Fujiwara, K., Taenaka, S., Otsushi, K., Yashima, A., Sawada, K., Hara, T., Ogawa, T. and Takeda, K. 2017. Study on coastal dyke reinforcement using double sheet-piles with partition walls, International Journal of Offshore and Polar Engineering, pp. 310-317.

Furuichi, H., Hara, T., Tani, M., Nishi, T., Otsushi, K., and Toda, K. 2015. Study on Reinforcement Method of Dykes by Steel Sheet-pile against Earthquake and Tsunami Disasters. Japanese Geotechnical Journal, Vol. 10, No. 4, pp. 583-594. (in Japanese)

Iai, S. 1988. Similitude for shaking table tests on soil-structure-fluid model in 1g gravitational field, Report of the Port and Harbor Research Institute, 27 (3), pp. 3-24.

LIQCA Liquefaction Geo-Research Institute (LIQCARI). 2015. Manual of LIQCA2D15・LIQCA3D15.

Oka, F., Yashima, A., Shibata, T., Kato., M. and Uzuoka, R. 1994. FEM-FDM coupled liquefaction analysis of a porous soil using an elasto-plastic model, Applied Scientific Research, 52, pp. 209-245.

Oka, F., Yashima, A., Tateishi, A., Taguchi, Y. and Yamashita, A. 1999. A cyclic elasto-plastic constitutive model for sand considering a plastic-strain dependence of the shear modulus, Geotechnique, 49 (5).

Oka, F., Yoshida, N., Kai, S., Tobita, T., Higo, Y., Torii, N., Kagamihara, S., Nakanishi, N., Kimoto, S., Yamakawa, Y., Touse, Y., Uzuoka, R. and Kyoya, T. 2012. Reconnaissance Report of Geotechnical Damage due to the 2011 off the Pacific coast of Tohoku Earthquake - Northern Area of Miyagi Prefecture -. Japanese Geotechnical Journal, Vol. 7, No. 1, pp. 37-55. (in Japanese)

Ramberg, W., Osgood, W, R. 1943. Description of stress–strain curves by three parameters, Technical Note No. 902, National Advisory Committee For Aeronautics.